

## A DC POLAROGRAPHIC STUDY OF THE REDUCTION OF OXYGEN CATALYZED BY ADSORBED Pb(II) SPECIES

M.M.J. PIETERSE, M. SLUYTERS-REHBACH and J.H. SLUYTERS

*Van 't Hoff Laboratory, State University, Padualaan 8, 3584 CH Utrecht (The Netherlands)*

(Received 5th October 1979)

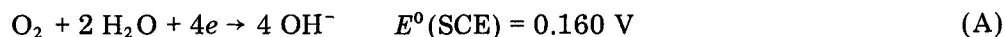
### ABSTRACT

The enhancement of the dc polarographic reduction current of oxygen by adsorbed Pb(II) species first observed by Strnad in 1939 and later studied qualitatively by a number of other authors has been reconsidered both experimentally and theoretically.

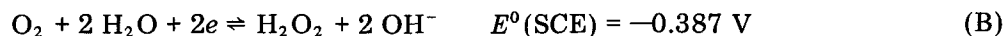
A number of possible reaction mechanisms is considered. The experimental results obtained in this work could be fitted well only to one of these mechanisms. It is concluded that the activation energy of the electrochemical reduction of  $\text{H}_2\text{O}_2$  to  $\text{OH}^-$  ions is lowered by an amount proportional to the surface excess of the Pb(II) species and that the participation of a Pb(II)–Pb(IV) oxidation-reduction cycle should be regarded as disproved.

### INTRODUCTION

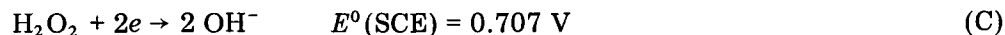
It is generally known that the electrochemical reduction of oxygen from aqueous solutions usually proceeds as a four-electron transfer, e.g. in alkaline medium according to:



Only in the case of special electrode materials being applied, like mercury and glassy carbon [1], the electrochemical reduction proceeds via two well-separated two-electron processes, the first one corresponding to:



and the second one corresponding to:



From the values of the standard potentials of these two reactions it must be concluded that from a thermodynamic point of view hydrogen peroxide,  $\text{H}_2\text{O}_2$ , is unstable and that its production on mercury and glassy carbon is possible only because of the highly irreversible nature of reaction (C). The behavior at the other metal electrodes like platinum and nickel is sometimes ascribed to the catalytic activity of the surface towards the disproportionation reaction:



The above reactions are all denoted for alkaline medium, but similar arguments hold for the corresponding reactions in acid medium involving free pro-

tons. Also, the partial dissociation of  $\text{H}_2\text{O}_2$  to  $\text{HO}_2^-$  at high pH is not relevant in this aspect.

Mercury and glassy carbon can be given catalytic activity as for the complete reduction by adding certain compounds which are most probably adsorbed at the electrode surface. In 1937 this was observed by Brdicka and Tropp [2] for small additions of a natural metal-chelate complex like hemoglobin. The reported effect appeared to depend on the catalyst concentration analogously to a Langmuirian isotherm [3]. Polarographic reduction of oxygen in the presence of other natural or synthetic catalysts is still a topical subject [4]. Of the latter class the metal (iron or cobalt)  $\text{N}_4$ -chelating agents such as phthalocyanines or porphyrins are being studied extensively. For a review see ref. [5].

Many simple inorganic substances like oxide suspensions, sols and metal ions also exhibit catalytic activity for the decomposition of  $\text{H}_2\text{O}_2$ , electrogenerated (in some nascent state?) at the dropping mercury electrode (DME) [3]. Detailed studies have been made by Strnad [3] and Arévalo and Bazo [6] of the most active compound, the Pb(II) species. Addition of small quantities ( $10^{-5}$ – $10^{-4}$  M) of Pb(II) causes an enhancement of the first two-electron oxygen wave. On further increase of the Pb(II) concentration the wave attains twice its original limiting current and appears to correspond to a single four-electron process. The effect is suddenly disrupted at the potential where Pb(II) is reduced to Pb(Hg). Furthermore, the catalytic activity is pH-dependent, being absent both at low pH, where the lead is mainly present as  $\text{Pb}^{2+}$ , and at high pH, where the  $\text{HPbO}_2^-$  ion is the predominant species. This suggests that the active species is a particular lead-hydroxo complex, most probably the neutral mononuclear  $\text{Pb}(\text{OH})_2$  [7].

The aim of this work is to explore the applicability of one or more theoretical models for the mathematical description of the Pb(II)-catalyzed oxygen reduction in terms of a dc current-voltage relationship. We hope that such a model can contribute to a better understanding of the part played by the electrode material in the electrochemistry of oxygen. The relationship should well describe the shapes and shifts of the first oxygen wave obtained from an air-saturated alkaline  $\text{KNO}_3$  solution (pH 12.35) to which increasing amounts of Pb(II) have been added. The high pH is chosen because in this medium the original wave is dc reversible [8,9].

In order to obtain an idea of the extent of the Pb(II) adsorption and its possible relation to the catalysis, the double-layer capacity of the DME employed, has been measured in the potential range where the effects are observed, at some Pb(II) concentrations and in the absence of air.

## EXPERIMENTAL

All experiments were performed at  $25.0^\circ\text{C}$  in a three-electrode cell. The working electrode was a DME with a sharp drawn-out capillary and a mercury pool served as the counter electrode. The reference electrode was a saturated calomel electrode (SCE) connected to the cell via a salt bridge filled with cell solution.

The cell solution consisted of 1 M  $\text{KNO}_3$  in twice-distilled water. The pH was made equal to 12.35 by adding KOH.  $\text{Pb}(\text{NO}_3)_2$  was added in small

aliquots from a 0.01 M + 1 M  $\text{KNO}_3$  stock solution to obtain the desired Pb(II) concentrations.

All chemicals were analytical grade. The solutions always remained clear during the experiment and the pH was constant. From stability constants [10] it can be calculated that the Pb(II) is present in our solution as the following species:  $\text{Pb}(\text{OH})^+$  0.1%;  $\text{Pb}(\text{OH})_2$  13.7%;  $\text{Pb}(\text{OH})_3^-$  86.2%.

The capacitance measurements were performed with our automatic network analyzer system [11] with an alternating voltage of 10 mV peak-to-peak at a frequency of 1000 Hz. The dc polarograms were recorded manually, making use of a potentiostat identical to that at present in use in the network analyzer system. The dc potential was controlled within 0.1 mV and the instantaneous dc current was measured with an accuracy better than 0.1%. The measurements were taken at 3.0 s after drop fall.

The oxygen concentration was fixed at 0.2 mM [9,12] by equilibrating the cell solution with air.

## RESULTS

### *The capacitance measurements*

The ac measurements were performed in the potential region limited at the anodic side ( $-100$  mV) by the oxidation of mercury to  $\text{HgO}$ , and at the cathodic side (about  $-600$  mV) by the start of the reduction of the Pb(II). The obtained values of the differential double-layer capacity  $C_d$  at Pb(II) concentrations ranging from 0 to 1 mM are reproduced in Fig. 1.

The effects of Pb(II) in the present deaerated solution are much larger than in the previously studied neutral 1 M KCl solutions [13,14] and are more like the effect of In(III) ions on the double-layer capacity at mercury in 1 M KCNS [15]. Evidently the adsorption of Pb(II) from the alkaline  $\text{KNO}_3$  solution may be considered as "strong" [15].

A most peculiar phenomenon in Fig. 1 is that the capacities are lowered on

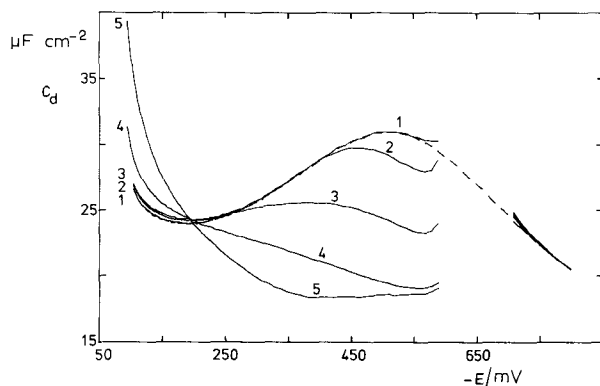


Fig. 1. Differential double-layer capacitance vs. potential curves of the Hg/1 M  $\text{KNO}_3$  + 0.04 M KOH (pH = 12.35) solution interface (dashed line) and with Pb(II): (1) 0.2; (2) 0.45; (3) 0.6; (4) 0.8; (5) 1.05 mM. Frequency = 1000 Hz.

addition of Pb(II) in the more negative potential region between  $-200$  and  $-600$  mV, but are raised in the potential region positive to  $-200$  mV. The "isosbestic point" [where apparently the Pb(II) does not influence the measured capacity value] closely resembles the common intersection point observed earlier in the  $C_d$  vs.  $E$  curves for solutions at different temperatures [16].

The qualitative conclusions to be drawn are that the Pb(II) adsorption probably increases towards more negative potentials (the electrocapillary maximum of mercury in  $1 M KNO_3$  is about  $-560$  mV vs. SCE [17]) and probably involves the neutral  $Pb(OH)_2$  and one or more charged complexes such as  $Pb(OH)_3^-$  (or  $HPbO_2^-$ ).

### The dc polarography of oxygen

Figures 2A and 2B show the polarograms of oxygen in the absence of lead (dots) and those with added lead at different concentrations ranging from 0.2

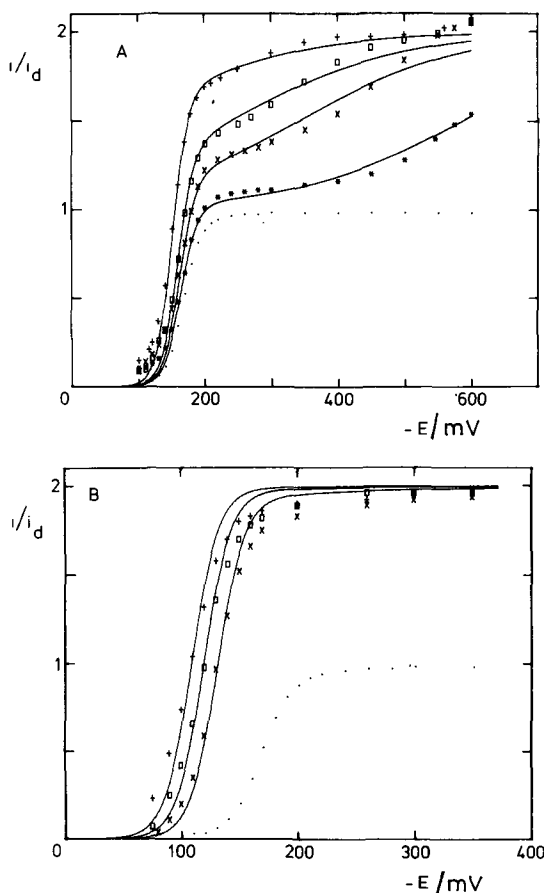


Fig. 2 (A). Normalized experimental (symbols) and theoretical (eqn. (26)) polarograms of the reduction of oxygen in a  $1 M KNO_3 + 0.04 M KOH$  ( $pH = 12.35$ ) solution and in the presence of Pb(II): ( $\cdot$ ) 0; ( $*$ ) 0.2; ( $\times$ ) 0.3; ( $\square$ ) 0.45; ( $+$ ) 0.6 mM. (B). As Fig. 2(A) with ( $\cdot$ ) 0; ( $\times$ ) 0.8; ( $\square$ ) 0.9; ( $+$ ) 1.05 mM.

to 1.05 mM. The polarograms are normalized by dividing the measured current by the limiting current  $i_d$  of the polarogram without lead. The half-wave potential of the uncatalyzed polarogram is  $-168$  mV vs. SCE.

In Figure 2A it is observed that the limiting current of the first oxygen wave increases on addition of Pb(II), and simultaneously the half-wave potential is shifted to a more positive value. At more negative potentials a further enhancement of the current is observed, increasing with decreasing potential more or less like a second wave. If the Pb(II) concentration is sufficiently high (0.6 mM) it can be seen that the current asymptotically approaches a limiting value twice the original limiting current. This tendency is demonstrated more clearly in Fig. 2B for the highest Pb(II) concentrations. The reduction wave of the Pb(II) itself, which starts at  $-600$  mV, is not shown here.

The waves in Fig. 2B apparently correspond to a single (reversible?) four-electron transfer reflecting the complete reduction of oxygen to water. However, the shift of the half-wave potential still continues. To our knowledge this phenomenon has not been previously reported.

It must be noted that the polarograms shown have not been corrected for charging currents. At the smaller current densities this may cause some error in the calculations to follow.

## THEORY

In a recent paper [9] we made a study of the reduction of oxygen to hydrogen peroxide (reaction B) at pH = 12.35 by means of impedance measurements. It was found that the charge-transfer process could be described by a rate equation of the Butler–Volmer type:

$$i_{O_2} = 2Fk_{sh,1} [c_R \exp(\alpha_{a,1} \phi_1) - c_O \exp(-\alpha_{c,1} \phi_1)] \quad (1)$$

with

$$\phi_1 = (2F/RT)(E - E_1^0) \quad (2)$$

The meaning of the other symbols is as follows:  $i_{O_2}$  is the current density due to reduction of  $O_2$  to peroxide;  $c_O$  the surface concentration of  $O_2$ ;  $c_R$  the sum of surface concentrations of  $H_2O_2$  and  $HO_2^-$ ;  $k_{sh,1}$  the standard heterogeneous rate constant, pertaining to  $E_1^0$ , i.e. the Nernst potential for  $c_O = c_R$ ; and  $\alpha_{c,1} = 1 - \alpha_{a,1}$  the cathodic transfer coefficient. The values obtained for  $\alpha_{c,1}$  and  $k_{sh,1}$  suggest that probably the first electron transfer,  $O_2 + e \rightleftharpoons O_2^-$  is rate-determining.

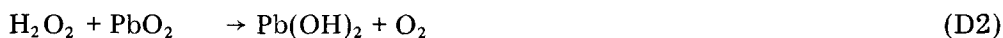
The rate of the overall reaction is so fast that the dc polarogram attains the "reversible shape", i.e. the dc current is controlled only by the diffusional mass transport.

The chemical decomposition of hydrogen peroxide, catalyzed by divalent and quadrivalent lead compounds has been studied by several authors [18–21], but it is hard to deduce an unambiguous reaction mechanism from these publications. From the reported observations some qualitative conclusions can be drawn:

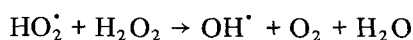
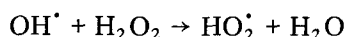
(a) hydrogen peroxide is able to oxidize Pb(II) with the formation of solid  $PbO_2$  (or  $Pb_3O_4$ ) and  $OH^-$  [7,18,21];

(b) hydrogen peroxide is able to reduce  $\text{PbO}_2$  with the formation of  $\text{Pb(II)}$  and  $\text{O}_2$  [17,19–21].

In view of this it is attractive to adopt an oxidation-reduction cycle between  $\text{Pb(II)}$  and  $\text{Pb(IV)}$ , ultimately leading to disproportionation of  $\text{H}_2\text{O}_2$  or  $\text{HO}_2^-$  as a possible mechanism [3], e.g.:



or similar reactions involving  $\text{HO}_2^-$  instead of  $\text{H}_2\text{O}_2$ , or a different  $\text{Pb(II)}$  species. Because of the fast association–dissociation equilibria, the actual notation is naturally trivial. It should be realized, however, that the reactions above may, or most probably will, involve partial steps, involving radicals such as  $\text{OH}^\cdot$  and  $\text{HO}_2^\cdot$ , which are known to be catalysts themselves for the decomposition of hydrogen peroxide [6,22], e.g. in the well-known Haber–Weiss cycle [23]:



Moreover, in our case it is not unlikely that these radicals, and also the quadrivalent lead, can be reduced electrochemically at the polarized mercury electrode, thus giving rise to the concomitant current. In the following sections we will discuss some of the possibilities in terms of their possible effects on the dc polarogram.

#### *Chemical decomposition of $\text{H}_2\text{O}_2$ leading to regeneration of $\text{O}_2$*

If we assume that the mechanism represented above by the reactions D1 and D2 take place at the electrode surface via adsorbed  $\text{Pb(OH)}_2$  or  $\text{PbO}_2$ , the enhanced current will be produced by the  $\text{O}_2$  which is formed in reaction D2, additional to the  $\text{O}_2$  flux. In the stationary state it can be postulated that the sum of the surface excesses  $\Gamma_{\text{Pb(OH)}_2} + \Gamma_{\text{PbO}_2} = \Gamma$  is constant and equal to the original amount of adsorbed lead. From the standard potentials of the redox couples involved it can be concluded that both the reactions D1 and D2 have a strongly one-sided equilibrium, so that their rates can be expressed by

$$v_1 = k'_1 \Gamma_{\text{Pb(OH)}_2} (\bar{c}_{\text{H}_2\text{O}_2} + \bar{c}_{\text{HO}_2^-}) = k_1 \bar{c}_R \quad (3)$$

$$v_2 = k'_2 \Gamma_{\text{PbO}_2} (\bar{c}_{\text{H}_2\text{O}_2} + \bar{c}_{\text{HO}_2^-}) = k_2 \bar{c}_R \quad (4)$$

where  $\bar{c}_i$  represents the dc surface concentration of the species concerned. As for the overall rate  $v$  two “submechanisms” may be distinguished, namely:

(1) The first step D1 is rate-determining: one has  $v_2 = v_1 = v$ , so that  $k_2 = k_1$ ; in the stationary state  $\Gamma_{\text{Pb(OH)}_2}$  and  $\Gamma_{\text{PbO}_2}$  will have a fixed ratio, which means that surface excesses are independent of time.

(2) The second step D2 is rate-determining: one has  $v = v_2 \neq v_1$ , and  $k_2 < k_1$ ;  $\Gamma_{\text{Pb(OH)}_2}$  will decrease as a function of time and  $\Gamma_{\text{PbO}_2}$  will increase accordingly. Note that the effect of this is a gradual increase of  $v_2$  with time which could eventually lead to the situation described under (1).

The fluxes of O (oxygen) and R (peroxide) to and from the interface must account for the rates of consumption and/or production of O and R, both by the electrochemical current and the reaction rates of D1 and D2. This is expressed by the flux equations:

$$D_O(\partial c_O/\partial x)_{x=0} = -(i_{O_2}/2F) - v_2 \quad (5a)$$

$$D_R(\partial c_R/\partial x)_{x=0} = (i_{O_2}/2F) + (v_1 + v_2) \quad (5b)$$

where  $D_O$  and  $D_R$  are the (mean) diffusion coefficients of O and R. A rigorous solution of Fick's second law with these boundary conditions, e.g. following the procedures proposed by Guidelli [24] seems possible, but for our purpose it will be sufficient to employ the approximate procedure, which for the DME leads to an explicit expression for the gradients [24]:

$$(\partial c_i/\partial x)_{x=0} = (c_i^* - \bar{c}_i)(3\pi t D_i/7)^{-1/2} \quad (6)$$

where  $t$  is the electrolysis time and  $c_i^*$  the concentration in the bulk. It was shown recently [25,26] that this so-called diffusion layer approximation is quite satisfactory to describe the shape of a dc polarogram in the case of reactant adsorption, the aspects of which have much in common with the present problem.

The current density  $i_{O_2}$  has already been specified in eqn. (1) but, because of the dc reversible behaviour this equation may be replaced by the Nernst equation in the form:

$$\bar{c}_O D_O^{1/2}/\bar{c}_R D_R^{1/2} = (D_O^{1/2}/D_R^{1/2}) \exp(\phi_1) = \exp(j) \quad (7)$$

From eqns. (5)–(7) with  $c_R^* = 0$  the following implicit expression for the current density  $i = i_{O_2}$  can be derived:

$$\begin{aligned} (i/2F)[1 + \exp(j)] &= -c_O^* D_O^{1/2} (3\pi t/7)^{-1/2} - v_2 - (v_1 + v_2) \exp(j) \\ &= i_d/2F - v_2 - (v_1 + v_2) \exp(j) \end{aligned} \quad (8)$$

where  $i_d$  denotes the limiting current of the first dc polarographic wave of oxygen in the absence of the catalytic process. From eqns. (3)–(7) it can be derived that

$$v_1 = (k_1/k_2)v_2 = \frac{c_O^* D_O^{1/2}}{(3\pi t/7)^{1/2} + (D_R^{1/2}/k_1)[1 + \exp(j)]} \quad (9)$$

which gives for the explicit equation of the dc polarogram:

$$\frac{i}{i_d} = \frac{1 + (k_1 + k_2)(3\pi t/7D_R)^{1/2}}{1 + \exp(j) + k_1(3\pi t/7D_R)^{1/2}} \quad (10)$$

In view of the mechanism of the  $O_2/H_2O_2$  electrode reaction itself [9] it could be more plausible that in the regeneration step (D2) the peroxide is only partly oxidized, e.g. to the  $HO_2$  radical, which thereafter is electrochemically reduced by one electron. A derivation similar to that given above leads then to an almost identical equation:

$$\frac{i}{i_d} = \frac{1 + (k_1 + \frac{1}{2}k_2)(3\pi t/7D_R)^{1/2}}{1 + \exp(j) + k_1(3\pi t/7D_R)^{1/2}} \quad (10a)$$

In addition, it could be supposed that in the "splitting step" (D1) the  $\text{H}_2\text{O}_2$  is partly reduced to  $\text{OH}^-$  and  $\text{OH}^\cdot$  and that the latter is further reduced by a fast uptake of an electron from the electrode. The flux equations for this case read:

$$D_{\text{O}}(\partial c_{\text{O}}/\partial x)_{x=0} = -i_{\text{O}_2}/2F \quad (11a)$$

$$D_{\text{R}}(\partial c_{\text{R}}/\partial x)_{x=0} = (i_{\text{O}_2}/2F) + v_1 \quad (11b)$$

The total current  $i = i_{\text{O}_2} + i_{\text{HO}_2^\cdot} + i_{\text{OH}^\cdot} = i_{\text{O}_2} - F(v_2 + v_1)$  is then given by

$$\frac{i}{i_{\text{d}}} = \frac{1 + [k_1 + \frac{1}{2}(k_1 + k_2)](3\pi t/7D_{\text{R}})^{1/2}}{1 + \exp(j) + k_1(3\pi t/7D_{\text{R}})^{1/2}} \quad (10b)$$

The conclusion is that these alternative possibilities cannot be distinguished from one another.

If a polarographic wave obeys eqn. (10), the values of  $k_1$  and  $k_2$  can easily be determined from the following characteristics:

(1) For  $\exp(j) \ll 1$  the current attains a limiting value  $i_{\text{L}}$ , given by

$$\frac{i_{\text{L}}}{i_{\text{d}}} = 1 + \frac{k_2(3\pi t/7D_{\text{R}})^{1/2}}{1 + k_1(3\pi t/7D_{\text{R}})^{1/2}} \quad (12)$$

(2) A "log-plot" of  $(i_{\text{L}} - i)/i$  vs. potential must yield a straight line according to:

$$\frac{i_{\text{L}} - i}{i} = \frac{\exp(j)}{1 + k_1(3\pi t/7D_{\text{R}})^{1/2}} \quad (13)$$

(3) Equation (13) explains the positive shift of the half-wave potential, since  $i = \frac{1}{2}i_{\text{L}}$  at

$$E_{1/2} = E^0 + (RT/2F) \ln(D_{\text{R}}/D_{\text{O}})^{1/2} + (RT/2F) \ln[1 + k_1(3\pi t/7D_{\text{R}})^{1/2}] \quad (14)$$

(4) The enhanced current  $i$  becomes equal to the original limiting current  $i_{\text{d}}$  (in the absence of the catalyst) at the potential

$$E_{i=i_{\text{d}}} = E^0 + (RT/2F) \ln(D_{\text{R}}/D_{\text{O}})^{1/2} + (RT/2F) \ln[k_2(3\pi t/7D_{\text{R}})^{1/2}] \quad (15)$$

In Fig. 3 our experimental data are fitted to theoretical polarograms calculated from eqn. (10) with the values for  $k_1$  and  $k_2$  tabulated in Table 1. It is clear that in the potential region 0 to  $-250$  mV vs. SCE, the agreement is very good. The values of  $k_1$  and  $k_2$  for each  $\text{Pb(II)}$  concentration are almost the same, so that we could conclude that the catalytic mechanism D is applicable and that the first step (D1), is rate-determining. However, the concentration dependence of  $k_1$  is quite remarkable: instead of being linear, it appears that  $k_1$  is an exponential function of  $c_{\text{Pb(II)}}$ . To verify this,  $\log k_1$  is plotted against  $c_{\text{Pb(II)}}$  in Fig. 4.

This finding seems seriously to disprove the simple mechanism (D), as it suggests a linear relationship between the activation energy of the rate-determining step and  $\Gamma$  rather than the stoichiometric participation of the absorbed lead in the decomposition-regeneration cycle.

Moreover, in the case of the lower  $\text{Pb(II)}$  concentrations the current at the more negative potentials,  $< -350$  mV, is observed to increase beyond the limit-



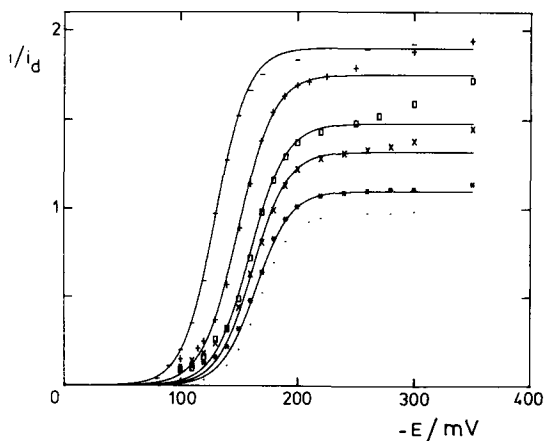


Fig. 3. Normalized experimental (symbols) and theoretical (eqn. (10)) polarograms of the reduction of oxygen and in the presence of Pb(II): (•) 0; (\*) 0.2; (x) 0.3; (□) 0.45; (+) 0.6; and (—) 0.8 mM. The values of  $k_1$  and  $k_2$  are given in Table 1.

TABLE 1

The experimental parameters  $k_1$  and  $k_2$

$c_{\text{Pb(II)}}/\text{mM}$	$10^4 k_1/\text{cm s}^{-1}$	$10^4 k_2/\text{cm s}^{-1}$
0	0	0
0.2	4.1	2.3
0.3	9.2	9.1
0.45	14.0	16.0
0.6	45.2	48.5
0.8	275	262
0.9	674	645
1.05	1746	1636

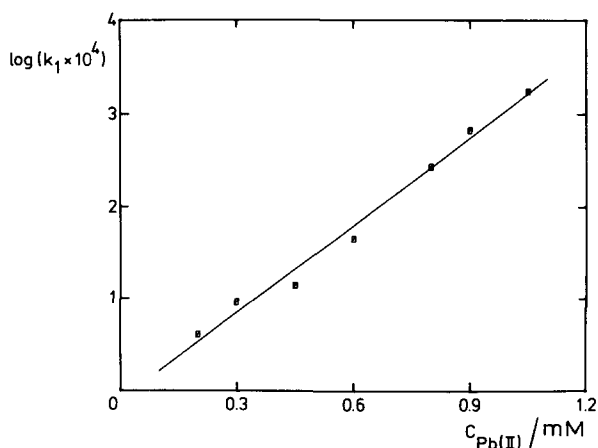


Fig. 4. The logarithm of the experimental parameter  $k_1$  as a function of the analytical Pb(II) concentration.

ing current corresponding to  $k_1$  and  $k_2$  in Table 1 (see Fig. 2). This could be related to the capacity curves in Fig. 1, which suggest that the adsorption of Pb(II) species increases towards more negative potentials. So, the rate constant of the catalyzed process is likely to be potential-dependent. Roughly, this could be visualized by still assuming that  $k_2 = k_1$  and calculating  $k_1$  with the aid of eqn. (10). The resulting  $\log k_1$  is plotted against potential in Fig. 5.

However, returning to the more general views at the beginning of this section, it should be examined whether another mechanism, involving potential dependency, could apply. This will be done in the next subsection.

*Chemical reaction of  $H_2O_2$  with Pb(II) followed by electrochemical reduction of Pb(IV)*

The mechanism to be treated is represented by the reactions:



The flux equations for this case are

$$D_O(\partial c_O/\partial x)_{x=0} = -i_{O_2}/2F \quad (16a)$$

$$D_R(\partial c_R/\partial x)_{x=0} = (i_{O_2}/2F) + v_1 \quad (16b)$$

The total current  $i = i_{O_2} + i_{PbO_2}$ , where  $i_{PbO_2}$  must be given by

$$i_{PbO_2} = -2Fk_f\Gamma_{PbO_2} = -2Fk_2(E) \quad (17)$$

where  $k_2(E)$  is a function of the potential  $E$ . As usual for an electrochemical reduction, it may be expected that the forward rate constant  $k_f$  increases expo-

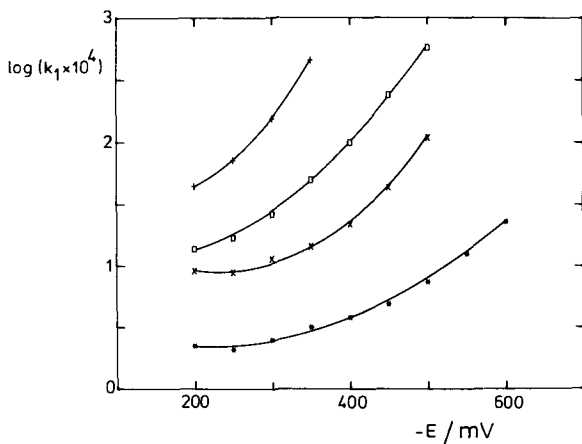


Fig. 5. The logarithm of the experimental parameter  $k_1$  as a function of the potential at different Pb(II) concentrations: (\*) 0.2; (x) 0.3; (□) 0.45; (+) 0.6 mM.

nentially with decreasing potential [e.g.  $d \ln k_f/dE = -\alpha(nF/RT)$ ]. Maintaining the assumptions underlying eqns. (6) and (7), we can derive the following expression for  $i/i_d$ :

$$\frac{i}{i_d} = \frac{1 + k_1(3\pi t/7D_R)^{1/2}}{1 + \exp(j) + k_1(3\pi t/7D_R)^{1/2}} + \frac{k_2(E)(3\pi t/7)^{1/2}}{c_O^*D_O^{1/2}} \quad (18)$$

in which  $k_1$ , the rate constant of reaction (E1), has the same meaning as before, cf. eqn. (3).

When considering the possible validity of eqn. (18), it must be stressed that this makes sense only if the second step (E2) is rate-determining. Otherwise, if (E1) is rate-determining,  $k_f\Gamma_{\text{PbO}_2} = v_2(E)$  will be equal to  $v_1$  and it is easily shown that eqn. (18) reduces to eqn. (10). So, the values of  $k_2(E)$  and  $k_1$  must obey the inequality

$$\frac{k_2(E)(3\pi t/7D_R)^{1/2}}{c_O^*(D_O/D_R)^{1/2}} < \frac{k_1(3\pi t/7D_R)^{1/2}}{1 + \exp(j) + k_1(3\pi t/7D_R)^{1/2}} \quad (19)$$

The first term in eqn. (18) in fact merely represents the oxygen reduction wave, shifted in a positive direction on the potential axis because of the occurrence of the "following reaction" (E1) which consumes the reduction product. If the second term, representing  $i_{\text{PbO}_2}/i_d$ , is postulated to be an exponential function of potential, the polarogram could be constructed as indicated in Fig. 6 from the two contributions. However, it is evident that, in view of the inequality (19), this is allowed only in the small potential region between  $-170$  and  $-260$  mV. It turns out that for none of the polarograms measured a reasonable combination of  $k_1$  and  $k_2(E)$  can be found to explain their shape in the whole potential region  $-100$  to  $-600$  mV.

#### *Electrochemical reduction of $H_2O_2$ , accelerated by adsorbed lead*

The models discussed above are based on the idea also postulated in the papers of Strnad [3] and Arévalo and Bazo [6], that the first step in the cata-

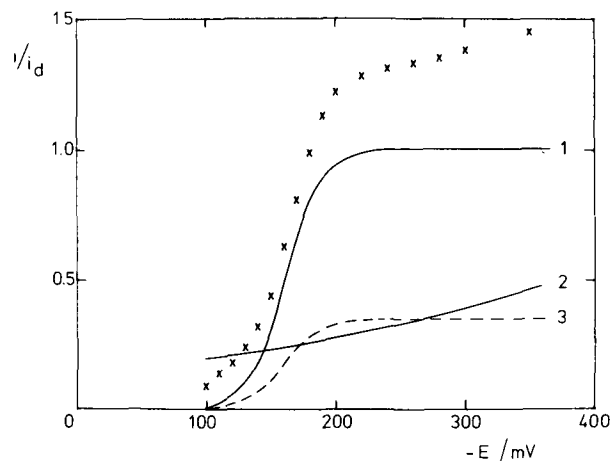


Fig. 6. Normalized experimental (x) polarogram [air-saturated + 0.3 mM Pb(II)] and theoretical polarograms: (1)  $i_{O_2}$ ; (2)  $i_{\text{PbO}_2}$ ; (3)  $v_1(3\pi t/7)^{1/2}/c_O^*D_O^{1/2}$ .

lytic process is the *chemical reduction* of  $\text{H}_2\text{O}_2$  by the adsorbed lead. However, in view of the second oxygen wave, obviously the  $\text{H}_2\text{O}_2$  can be reduced *electrochemically*, provided that the electrode potential of the DME is made sufficiently negative. To put it otherwise, the rupture of the O—O bond is achieved via an uptake of two electrons from the mercury, provided that the activation energy is lowered electrically.

In this subsection we will explore the possibility that this electrochemical process is accelerated for some reason by the presence of adsorbed lead. Since the second wave is highly irreversible, such an acceleration would, in the first instance, cause a shift of this wave towards positive potentials, i.e. towards the potential region of the first wave. If the effect is large, the two waves will overlap and the whole process has to be treated as occurring via the consecutive steps:



The flux equations for the participating species read:

$$D_{\text{O}}(\partial c_{\text{O}}/\partial x)_{x=0} = -i_{\text{O}_2}/2F \quad (20\text{a})$$

$$D_{\text{R}}(\partial c_{\text{R}}/\partial x)_{x=0} = (i_{\text{O}_2}/2F) - i_{\text{R}}/2F \quad (20\text{b})$$

where  $i_{\text{O}_2}$  is the current carried by reaction (B) and  $i_{\text{R}}$  is the current carried by reaction (C). Formally, also the flux equation for  $c_{\text{OH}^-}$  should be accounted for, but since in our solution  $c_{\text{OH}^-}^* \gg c_{\text{O}}^*$ , its surface concentration will not significantly differ from the bulk  $\text{OH}^-$  concentration. The rate equation for  $i_{\text{O}_2}$  has been given by eqn. (1) and a similar Butler—Volmer-type equation may be postulated for the second step, namely:

$$i_{\text{R}} = 2Fk_{\text{sh},2} [c_{\text{OH}^-}^2 \exp(\alpha_{\text{a},2}\phi_2) - c_{\text{R}} \exp(-\alpha_{\text{c},2}\phi_2)] \quad (21)$$

where again  $c_{\text{R}} = c_{\text{H}_2\text{O}_2} + c_{\text{HO}_2^-}$  and  $c_{\text{O}} = c_{\text{O}_2}$ .

A general theory for such a two-step multielectron electrode reaction has been developed by Ruzi'c [27]. Here we will briefly describe the derivation of the  $i - E$  characteristic for our present case, immediately introducing Nernstian conditions for the reaction (B), i.e. eqn. (7), the diffusion layer approximation, i.e. eqn. (6), and a more surveyable notation of eqn. (21):

$$i_{\text{R}} = 2Fk_{\text{f}} [(c_{\text{OH}^-}^*)^2 \exp(\phi_2) - \bar{c}_{\text{R}}] \quad (22)$$

with

$$\phi_2 = (2F/RT)(E - E_2^0) \quad (23)$$

The formal standard potential  $E_2^0$  can be derived from tabulated standard potentials for peroxide reduction in alkaline medium in a similar way as we did previously [9] for reaction (B); its value is about +724 mV vs. SCE.

Straightforward combination of eqns. (6), (7), (20) and (22) enables elimination of the surface concentrations  $\bar{c}_{\text{O}}$  and  $\bar{c}_{\text{R}}$  and leads to the following expres-

sions for  $i_{O_2}$  and  $i_R$ :

$$i_{O_2} = - \frac{2F}{(3\pi t/7)^{1/2}} \frac{c_O^* D_O^{1/2} (1 + a_R/k_f) - (c_{OH^-}^*)^2 D_R^{1/2} \exp(\phi_2 + j)}{1 + [\exp(j) + 1] a_R/k_f} \quad (24)$$

$$i_R = - \frac{2F}{(3\pi t/7)^{1/2}} \frac{c_O^* D_O^{1/2} - (c_{OH^-}^*)^2 D_R^{1/2} \exp(\phi_2) [\exp(j) + 1]}{1 + [\exp(j) + 1] a_R/k_f}$$

with  $a_R = (7D_R/3\pi t)^{1/2}$ . The total current is the sum of these two currents. Because of the highly positive  $E_2^0$ -value, the term containing  $\exp \phi_2$  can be neglected in our potential region. Consequently the expression for the total normalized current becomes

$$\frac{i}{i_d} = \frac{1 + 2k_f(3\pi t/7D_R)^{1/2}}{1 + \exp(j) + k_f(3\pi t/7D_R)^{1/2}} \quad (26)$$

which is of a form identical to eqn. (10), but now with a rate constant allowed to be potential-dependent, in a way corresponding to the Butler–Volmer equation, i.e.  $k_f = k_{sh} \exp(-\alpha\phi_2)$  [see eqns. (21) and (22)].

The usual log-plot analysis of the uncatalyzed  $H_2O_2$  reduction wave in the potential region  $-900$  to  $-1300$  mV vs. SCE yields the parameters  $k_{sh}^0 = 0.84 \times 10^{-9}$  cm s $^{-1}$  and  $\alpha = 0.107$ , with which the potential dependency of the forward rate constant  $k_f^0$  in the uncatalyzed case is determined.

An attempt to fit our experimental data to eqn. (26) with the same  $\alpha = 0.107$ , but with increased  $k_{sh}$ , led to the theoretical polarograms in Figs. 2A and 2B, where it can be seen that the shapes are in more or less reasonable agreement with the experimental points, but the deviations are nearly always beyond the experimental error. Therefore it is more useful to calculate  $k_f$  directly as a function of potential and try to interpret the results. In Fig. 7 the calculated  $\log k_f$

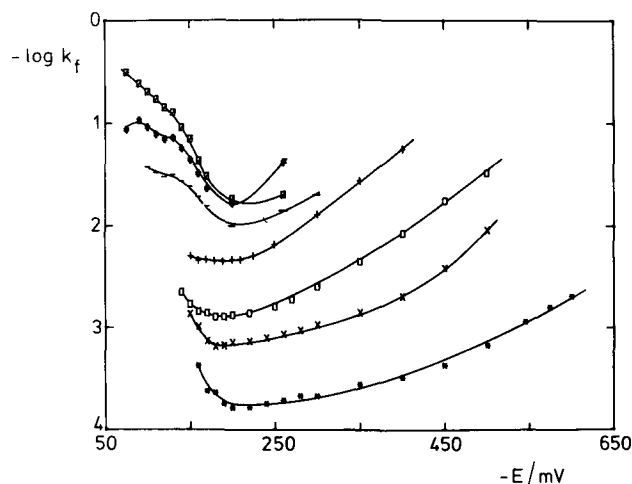


Fig. 7. The heterogeneous forward rate constant of the electrochemical reduction of  $H_2O_2$  in the presence of  $Pb(II)$  as a function of the potential. (\*) 0.2; (x) 0.3; ( $\square$ ) 0.45; (+) 0.6; (—) 0.8; (#) 0.9; ( $\square$ ) 1.05 mM.

is plotted against potential. Too inaccurate values have been omitted, so the observed bending of the curves is significant.

The behaviour of  $k_f$  in the potential region  $E < -200$  mV is "normal" in this sense that it increases with decreasing potential and that it strongly increases with the Pb(II) concentration. The value of  $\alpha$  (defined as  $-(RT/nF) d \ln k_f/dE$ ) is not constant, but increases from zero at  $E = \text{ca. } -200$  mV to 0.17–0.19 in the final 100 mV region of each curve. So the apparent transfer coefficient is of the same order of magnitude as that for the uncatalyzed case, but most probably the catalyzing effect itself is potential-dependent because of potential dependency of the Pb(II) adsorption.

The behaviour of  $k_f$  in the potential region  $E > -200$  mV is most remarkable, because the apparent  $\alpha$  is found to be negative. It must be concluded that either the mechanism changes drastically in the region where the first reduction step is not complete (i.e.  $\bar{c}_O$  at the electrode surface is not equal to zero), or the species responsible for the acceleration of the  $\text{H}_2\text{O}_2$  reduction is different. As regards the latter possibility it must be noticed that the inflection of the  $\log k_f$  vs.  $E$  curve occurs at the same potential,  $-200$  mV, where the capacity curves in Fig. 1 have their common intersection point. It is not unlikely that at  $E > -200$  mV the charged species  $\text{HPbO}_2^-$  is adsorbed preferentially to the neutral  $\text{Pb(OH)}_2$ .

Many examples are known of heterogeneous rate constants being increased (or decreased) by charged or uncharged adsorbates. Usually an attempt is made to relate the observations to a simple model in which a linear relation is postulated between the surface coverage  $\theta$  and either the rate constant itself, or its logarithm [28]. The latter possibility is tested here by considering the relation

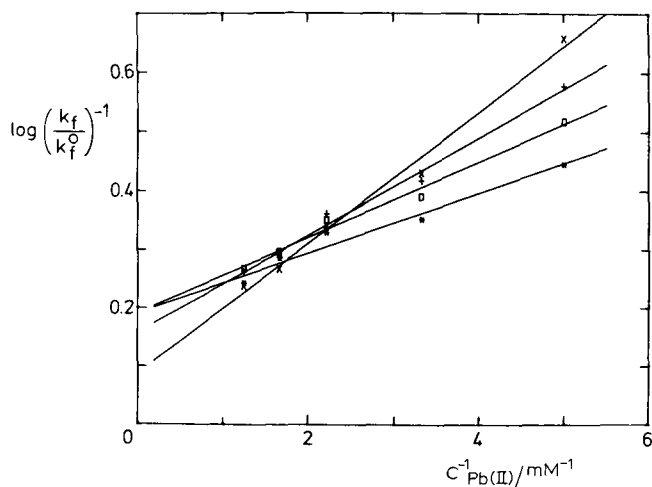


Fig. 8. The heterogeneous forward rate constants of the electrochemical reduction of  $\text{H}_2\text{O}_2$  in the presence ( $k_f$ ) and without Pb(II) ( $k_f^0$ ) as a function of the reciprocal value of the analytical Pb(II) concentrations at different potentials. (\*)  $-170$ ; ( $\square$ )  $-200$ ; (+)  $-300$ ; and ( $\times$ )  $-400$  mV.

[29]:

$$\log k_f(E) - \log k_f^0(E) = [\log k_f^m(E) - \log k_f^0(E)] \theta \quad (27)$$

where  $k_f^0$  pertains to zero Pb(II) concentration, and  $k_f^m$  must represent the rate constant pertaining to monolayer coverage ( $\theta = 1$ ). If the adsorption obeys a Langmuir isotherm, one has  $\theta = \beta c / (1 + \beta c)$ , where  $\beta$  is the adsorption coefficient. A plot of  $1/\log(k_f/k_f^0)$  against  $1/c_{\text{Pb(II)}}$  must then be linear. This is checked in Fig. 8 at four different potentials. Linearity is fairly well achieved and the slopes are systematically different.

From these plots the following values for  $\beta$  can be estimated:

-170 mV	$\beta = 2.6 \times 10^5 \text{ cm}^3 \text{ M}^{-1}$
-200 mV	$\beta = 3.2 \times 10^5 \text{ cm}^3 \text{ M}^{-1}$
-300 mV	$\beta = 4.7 \times 10^5 \text{ cm}^3 \text{ M}^{-1}$
-400 mV	$\beta = 1.1 \times 10^6 \text{ cm}^3 \text{ M}^{-1}$

These values have a realistic order of magnitude and are indeed significantly potential-dependent.

## CONCLUSIONS

The normal mechanism by which a catalyst is believed to work is that it offers an alternative pathway for the reaction with a lower activation energy, leading to an increase of the overall reaction rate proportional to the amount of catalyst present.

However, the enhancement of the faradaic oxygen reduction current by adsorbed Pb(II) species appears to be due to a lowering of the activation energy of the electrochemical  $\text{H}_2\text{O}_2$  reduction reaction, the amount with which this activation energy is lowered being proportional to the surface excess of the Pb(II) species. The rate constant of the  $\text{H}_2\text{O}_2$  reduction has been found to have increased at least by a factor of  $10^5$  by the adsorption of half a monolayer of Pb(II). Also it is probable that the nature of the active Pb(II) species is potential-dependent.

These conclusions are incompatible with a mechanism involving the oxidation-reduction cycle of Pb(II)—Pb(IV) usually adopted or with an explanation involving active sites.

## ACKNOWLEDGEMENT

The authors wish to express their gratitude to Mr. A.G. Remijnse for carrying out the capacity measurements.

## REFERENCES

- 1 J.P. Hoare, *The Electrochemistry of Oxygen*, Interscience, New York, 1968.
- 2 R. Brdicka and C. Tropp, *Biochem. Z.*, 289 (1937) 301.
- 3 F. Strnad, *Collect. Czech. Chem. Commun.*, 11 (1939) 391.
- 4 G. Meyer and M. Savy, *Electrochim. Acta*, 22 (1977) 213.
- 5 H. Behret, W. Clauberg and G. Sandstede, *Ber. Bunsenges. Phys. Chem.*, 81 (1977) 54.
- 6 A. Arévalo and A. Bazo, in G.J. Hills (Ed.), *Polarography*, Macmillan, London, 1964, p. 457.

- 7 W.C. Schumb, C.N. Satterfield and R.L. Wentworth, *Hydrogen Peroxide*, Reinhold, New York, 1955, p. 480.
- 8 J. Kůta and J. Koryta, *Collect. Czech. Chem. Commun.*, **30** (1965) 4095.
- 9 M.M.J. Pieterse, M. Sluyters-Rehbach and J.H. Sluyters, *J. Electroanal. Chem.*, **107** (1980) 247.
- 10 L.G. Sillén and A.E. Martell, *Stability Constants*, The Chemical Society, London, 1964, p. 69.
- 11 C.P.M. Bongenaar, M. Sluyters-Rehbach and J.H. Sluyters, *J. Electroanal. Chem.*, **109** (1980) 23 (this issue).
- 12 C.G. MacArthur, *J. Phys. Chem.*, **20** (1915–16) 495.
- 13 B. Timmer, M. Sluyters-Rehbach and J.H. Sluyters, *J. Electroanal. Chem.*, **18** (1968) 93.
- 14 M. Sluyters-Rehbach, J.S.M.C. Breukel, K.A. Gijsbertsen, C.A. Wijnhorst and J.H. Sluyters, *J. Electroanal. Chem.*, **38** (1972) 17.
- 15 B. Timmer, M. Sluyters-Rehbach and J.H. Sluyters, *J. Electroanal. Chem.*, **15** (1967) 343; **19** (1968) 73.
- 16 B.G. Dekker, M. Sluyters-Rehbach and J.H. Sluyters, *J. Electroanal. Chem.*, **21** (1969) 137; D.C. Grahame, *J. Am. Chem. Soc.* **79** (1957) 2093.
- 17 J. Heyrovský and J. Kůta, *Principles of Polarography*, Academic Press, New York, 1966, p. 21.
- 18 U. Agarwala, M. Anbar and H. Taube, *J. Phys. Chem.*, **66** (1962) 1421.
- 19 M.M. Andrusev, A.A. Konoplina and L.A. Nikolaev, *Russ. J. Phys. Chem.*, **48** (1974) 694.
- 20 A.A. Konoplina, M.M. Andrusev and L.A. Nikolaev, *Russ. J. Phys. Chem.*, **49** (1975) 203.
- 21 K.G. Schick, V.G. Magearu, N.L. Field and C.O. Huber, *Anal. Chem.*, **48** (1976) 2186.
- 22 I.M. Kolthoff and F. Jordan, *J. Am. Chem. Soc.*, **74** (1952) 1071.
- 23 F. Haber and J. Weiss, *Proc. Roy. Soc.*, **A147** (1934) 332.
- 24 R. Guidelli, *J. Electroanal. Chem.*, **33** (1971) 291.
- 25 M. Sluyters-Rehbach, C.A. Wijnhorst and J.H. Sluyters, *J. Electroanal. Chem.*, **74** (1976) 3.
- 26 M. Sluyters-Rehbach and J.H. Sluyters, *J. Electroanal. Chem.*, **75** (1977) 371.
- 27 I. Ruzić, *J. Electroanal. Chem.*, **52** (1974) 331.
- 28 M. Sluyters-Rehbach and J.H. Sluyters, in A.J. Bard (Ed.), *Electroanalytical Chemistry*, Vol. 4, Marcel Dekker, New York (1966).
- 29 T. Biegler and H.A. Laitinen, *J. Electrochem. Soc.*, **113** (1966) 852.